Analysis of Dead Zone in RFID System

Mitsuo Taguchi(1) and Hiroyuki Mizuno(2)
(1) Dept. of Electrical & Electronic Eng., Nagasaki University
(2) Graduate School of Science & Technology, Nagasaki University
1-14 Bunkyo-machi, Nagasaki 852-8521, Japan
E-mail: (1) mtaguchi@net.nagasaki-u.ac.jp (2) d705102a@cc.nagasaki-u.ac.jp

***Abstract* — For the study on the dead zone in the RFID system, the electromagnetic field distribution near the finite conducting plate is calculated for the spherical wave incidence. The current distribution on the finite conducting plate is calculated by the integration of the current distributions due to the plane waves incident from different angles. In order to examine the validity of this plane wave expansion method, the electric field distribution near the conducting plane is compared with the calculated electric field distribution excited by the small dipole antenna.**

***Index Terms* — RFID system, dead zone, plane wave expansion.**

I. INTRODUCTION

Recently, the RFID (Radio Frequency Identification) systems have become very popular in many service industries, purchasing and manufacturing companies. When, however, the transponder without its own voltage supply is located near the conducting plate, the reader may not receive the ID signal from the transponder even it is within the interrogation zone of a reader. The authors have measured the dead zone in the RFID system [1].

In this paper, the dead zone in the RFID system is investigated. The current distribution induced on the square conducting plate is formulated as the integration of the current distribution due to the plane waves incident from different angles. The scattered electric field is calculated and discussed. The electric field distribution near the conducting plate is measured and the dead zone is discussed.

II. PLANE WAVE EXPANSION OF SPHERICAL WAVE

The scalar Helmholtz's equation is expressed in the spherical coordinate system as follows.

$$\frac{1}{r^2}\frac{\partial}{\partial r}(r^2\frac{\partial \psi}{\partial r})+\frac{1}{r^2\sin^2\theta}\frac{\partial^2\psi}{\partial\varphi^2}+\frac{1}{r^2\sin\theta}\frac{\partial}{\partial\theta}(\sin\theta\frac{\partial\psi}{\partial\theta})+k^2\psi=0 \tag{1}$$

If the solution of (1) is assumed as $\psi = R(r)\Theta(\theta)\Phi(\varphi)$, R, Θ and Φ satisfies each of the following differential equations[2].

$$\frac{d}{dr}(r^2\frac{dR}{dr})+\left\{k^2r^2-n(n+1)\right\}R=0 \tag{2}$$

$$\frac{1}{\sin\theta}\frac{d}{d\theta}(\sin\theta\frac{d\Theta}{d\theta})+\left\{n(n+1)-\frac{m^2}{\sin^2\theta}\right\}\Theta=0 \tag{3}$$

$$\frac{d^2\Phi}{d\varphi^2}+m^2\Phi=0 \tag{4}$$

Then, the general solution of (1) is expressed as

$$\psi_{m,n}=j_n(kr)P_n^m(\cos\theta)e^{jm\varphi} \tag{5}$$

where $j_n(r)$ is the spherical Bessel function of order n and $P_n^m(\cos\theta)$ is the associated Legendre polynomial. Plane wave is expressed by

$$e^{jz}=e^{jkr\cos\theta}=\sum_{n=0}^{\infty}a_n j_n(r)P_n(\cos\theta) \tag{6}$$

Where $P_n(u)$ is the Legendre polynomial.

$$P_n(u)=\frac{1}{2^n n!}\frac{d^n}{du^n}(u^2-1)^n$$

(6) is multiplied by $P_q(\cos\theta)\sin\theta$ and integrated from 0 to 2π.

$$\int_0^\pi e^{jr\cos\theta}P_n(\cos\theta)\sin\theta d\theta=\int_0^\pi a_n j_n(r)P_n(\cos\theta)P_q(\cos\theta)\sin\theta d\theta$$
$$=\frac{2a_n}{2n+1}j_n(r) \tag{7}$$

(7) is n times differentiated with respect to *r*, then

$$a_n=(2n+1)j^n \tag{8}$$

is obtained. Consequently, (7) becomes

$$j_n(r)=\frac{j^{-n}}{2}\int_0^\pi e^{jkr\cos\theta}P_n(\cos\theta)\sin\theta d\theta \tag{9}$$

The cylindrical wave is expressed in terms of the spherical wave.

$$J_0(\rho)=J_0(r\sin\theta)=\sum_{n=0}^{\infty}b_n j_{2n}(r)P_{2n}(\cos\theta) \tag{10}$$

Similar with the derivation of (7), the following equation is obtained.

$$\int_0^\pi J_0(r\sin\theta)P_{2n}(\cos\theta)\sin\theta d\theta=\frac{b_n}{4n+1}j_{2n}(r), \tag{11}$$

where

$$b_n=\frac{(-1)^n(4n+1)(2n-1)!}{2^{2n-1}n!(n-1)!} \tag{12}$$

Consequently, the following expression is obtained from (9), (11) and (12).

$$j_0(r)=\frac{\sin(r)}{r}=\frac{1}{4\pi}\int_0^\pi\int_0^{2\pi}e^{jr\cos\varphi\sin\theta}\sin\theta d\varphi d\theta \tag{13}$$

By replacing *r* to *r*+π/2, we obtain

$$y_0(r)=\frac{\sin(r+\frac{\pi}{2})}{r+\frac{\pi}{2}}=\frac{1}{4\pi}\int_0^\pi\int_0^{2\pi}e^{j(r+\frac{\pi}{2})\cos\varphi\sin\theta}\sin\theta d\varphi d\theta \tag{14}$$

Consequently, from (13) and (14) , we obtain the expression of spherical wave.

$$\frac{\exp(-jr)}{r} = \left(\frac{1}{4\pi} + \frac{1}{8r}\right)\int_0^{\pi}\int_0^{2\pi} e^{jr\cos\varphi\sin\theta} e^{j\frac{\pi}{2}\cos\varphi\sin\theta} \sin\theta d\varphi d\theta - j\frac{1}{4\pi}\int_0^{\pi}\int_0^{2\pi} e^{jr\cos\varphi\sin\theta}\sin\theta d\varphi d\theta \quad (15)$$

Fig. 1 shows the analytical model of spherical wave incidence. The spherical wave with horizontal polarization is incident to the square conducting plate of 60 cm by 60 cm. The frequency is 2.45 GHz.

The current distribution on the square conductor in the case of plane wave incidence is calculated by using the electromagnetic simulator WIPL-D based on the Method of Moment [3]. The incident angle is $0^{\circ} \le \theta \le 180^{\circ}$, $0^{\circ} \le \phi \le 180^{\circ}$. Let $\mathbf{J}(\theta, \phi)$ be the current distribution at the point (x, z) on the conducting plate due to the plane wave incident from (θ, ϕ), then the current distribution $\mathbf{J}_{sph}$ on the conducting plate in the case of spherical wave incidence is expressed by the plane wave expansion of spherical wave as follows.

$$\mathbf{J}_{sph} = \left(-\frac{k}{4\pi} + \frac{1}{8R}\right)\int_0^{\pi}\int_0^{\pi} \mathbf{J}(\theta,\phi)\exp\left(j\frac{\pi}{2}\cos\phi\sin\theta\right)\sin\theta d\phi d\theta - j\frac{k}{4\pi}\int_0^{\pi}\int_0^{\pi}\mathbf{J}(\theta,\phi)\sin\theta d\phi d\theta \quad (14)$$

The electric field distribution near the conducting plate is calculated by the integration of induced current on the conducting plate [4].

III. MEASUREMENT OF DEAD ZONE

Fig. 2 shows the experimental model of RFID system. The 4 by 4 square patch microstrip array antenna is used for the reader antenna. The operating frequency is 2.45 GHz. The reader antenna is located at the distance R from the center of conducting plate. As the passive transponder, the microstrip antenna with finite ground plane is used. The transponder is moved at the interval of 1 cm in the region of $-14\,\text{cm} \le x \le 36\,\text{cm}$, $0 \le z \le 45\,\text{cm}$ on the xz-plane. The reader reads the ID signal 256 times and records the detection error rate.

IV. RESULTS AND DISCUSSION

Fig. 3 shows the measured detection error rate without conducting plate for R=122cm. The incident angle is θ=0 deg. Fig. 4 shows the measured detection error rate for R=296cm and θ=0 deg. Fig. 5 shows the measured detection error rate for R=296cm and θ=30 deg. In Fig. 4 and Fig. 5, the white areas indicate the detection error rate greater than 20%. These areas are the dead zones.

In order to verify the proposed plane wave expansion method, the calculated scattered electric field distribution along the z axis is compared with the scattered electric field excited by the dipole antenna with its length of one hundredth located at the source point. Fig. 6 and 7 show the amplitude and phase distribution of scattered electric field on the z axis for R=60cm, respectively. Fig. 8 and 9 show the amplitude and phase distribution of scattered electric field distribution at y=1cm along the x direction, respectively. The scattered electric field distribution calculated from $\mathbf{J}_{sph}$ obtained by the plane wave expansion method agrees well with that excited by the small dipole antenna.

Figs. 10 and 11 show the electric field distribution on xz plane. Fig. 12 shows the magnetic field distribution on xz plane. From these figures, we can observe the dead zone near the conducting plate. The dead zone distribution is almost similar to the measured results shown in Figs. 4 and 5.

V. CONCLUSION

The dead zone in the RFID system has been numerically and experimentally investigated. The electromagnetic field distribution in the vicinity of square conducting plate has been examined in the case of spherical wave incidence. In the numerical analysis, the induced current on the conducting plate has been calculated from the current due to the incident plane wave by using the plane wave expansion of spherical wave. The scattered electric field distribution near the finite conducting plate has been obtained from the induced current on the conducting plate. The detection error rate of the RFID system has been measured.

The radiation field from the reader antenna can be expressed in terms of the spherical wave. Therefore the scattered electromagnetic field distribution is straightforwardly calculated from the induced current due to the incident plane wave.

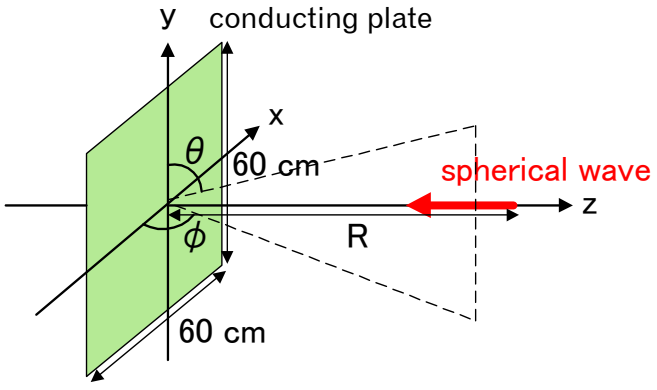

Fig. 1 Analytical model.

REFERENCES

[1] M. Taguchi and H. Mizuno: "Analysis of Dead Zone of RFID System", Proc. IEEE AP-S Int. Symp., July 2006.
[2] R. Harrington: "Time-harmonic electromagnetic fields", P. 289-316, McGraw-Hill, New York, 1961.
[3] http://www.wipl-d.com/
[4] S. Silver: "Microwave Antenna Theory and Design", p. 87, McGraw-Hill, 1947.

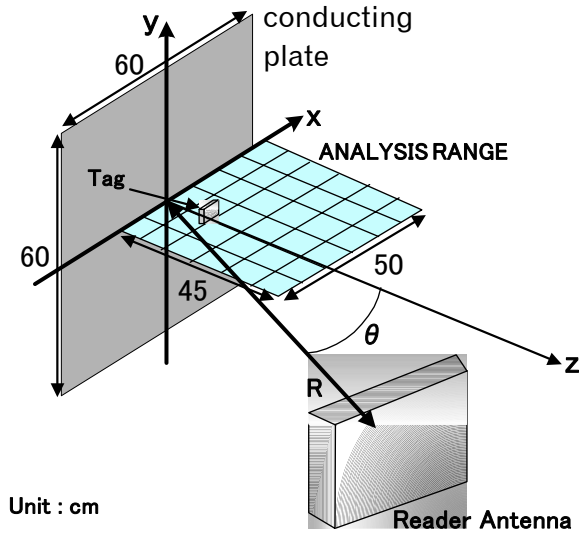

Fig. 2. Experimental model of RFID system.

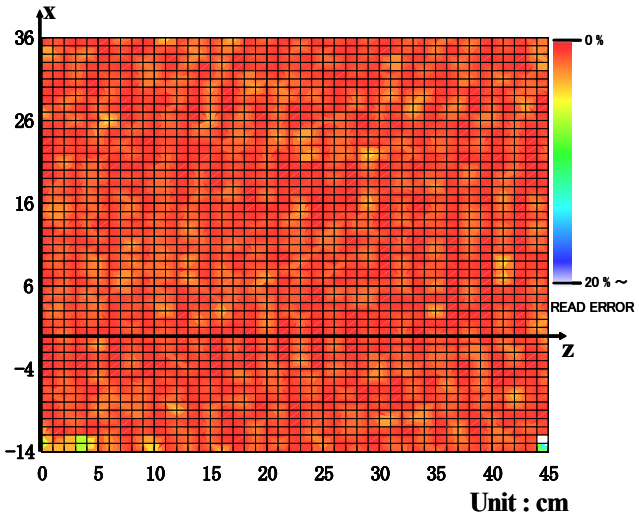

Fig. 3 Measured detection error rate without conductor. R=122cm, θ=0deg

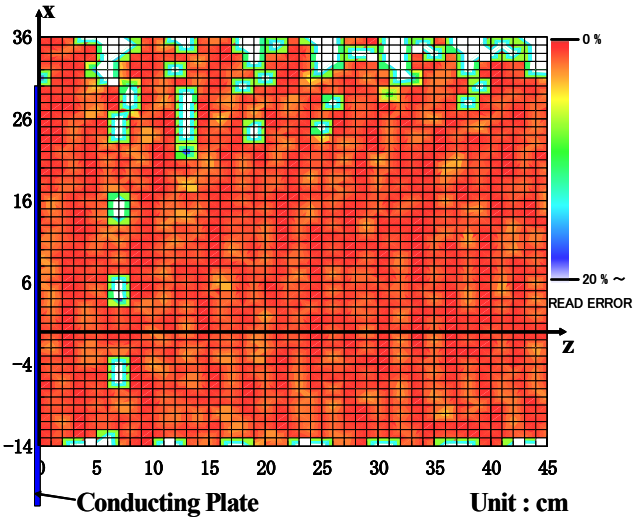

Fig. 4 Measured detection error rate. R=122cm, θ=0deg

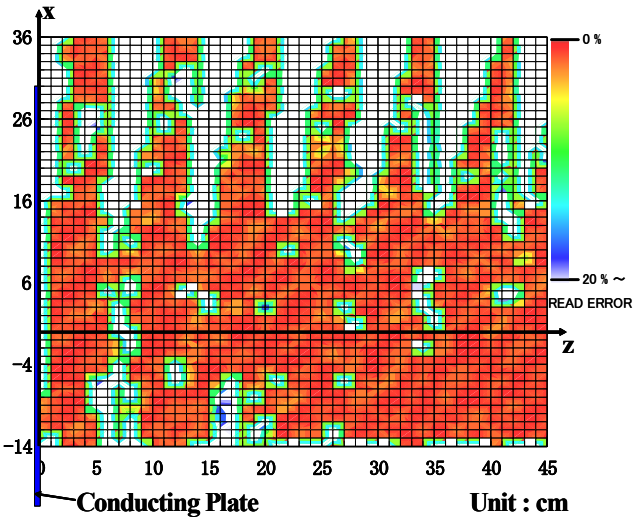

Fig. 5 Measured detection error rate. R=296cm, θ=0deg

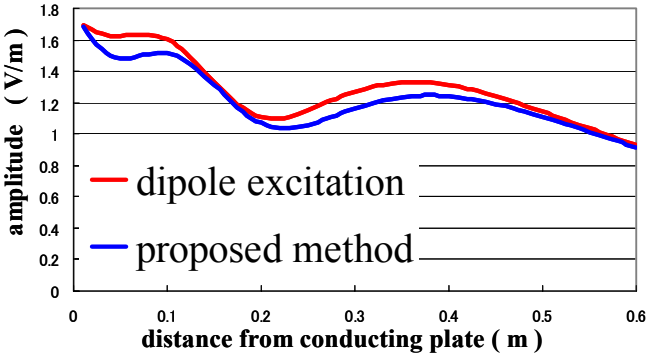

Fig. 6 Amplitude of scattered electric field on z axis.

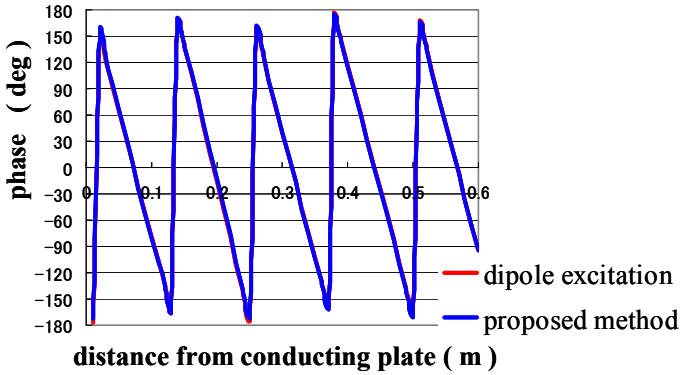

Fig. 7 Phase distribution of scattered electric field on z axis.

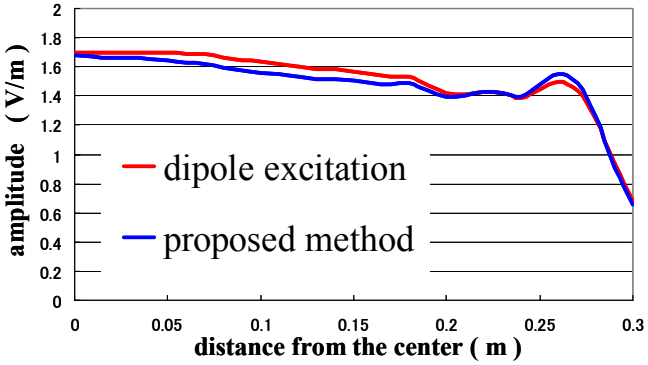

Fig. 8 Amplitude distribution of scattered electric field on x-axis at y=1cm.

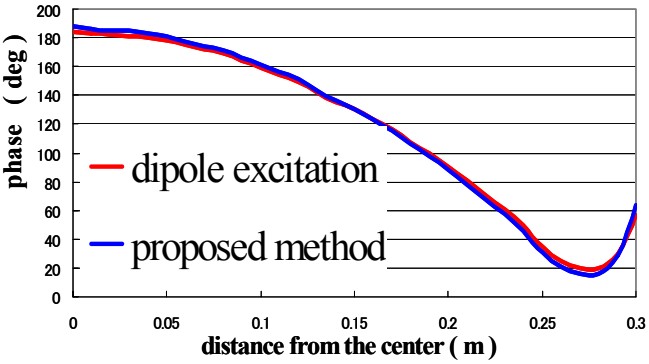

Fig. 9 Phase distribution of scattered electric field on x-axis at y=1cm.

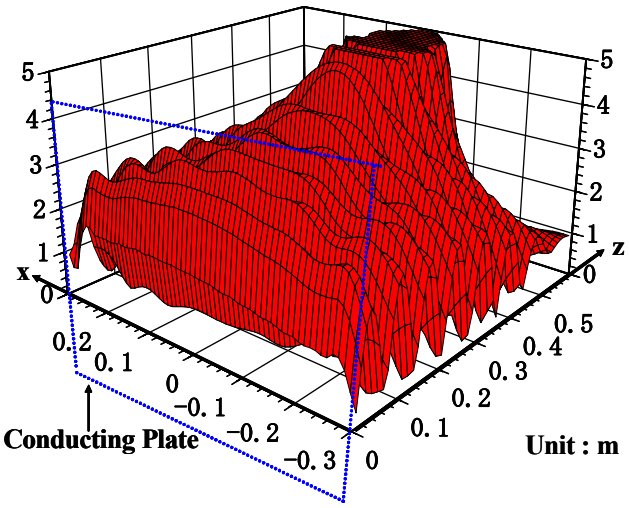

Fig. 10 Electric field distribution in xz plane.

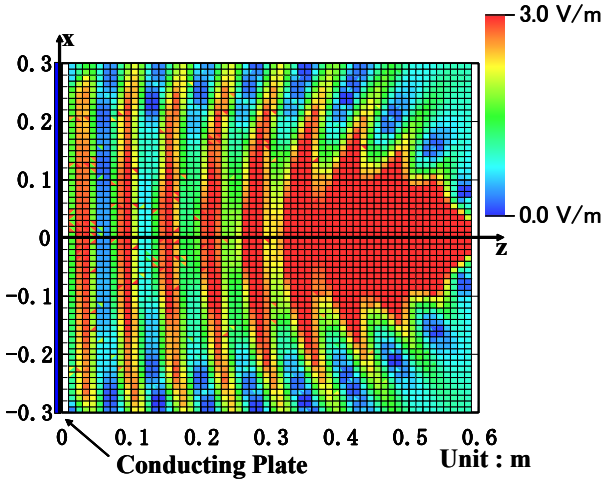

Fig. 11 Electric field distribution in xz plane.

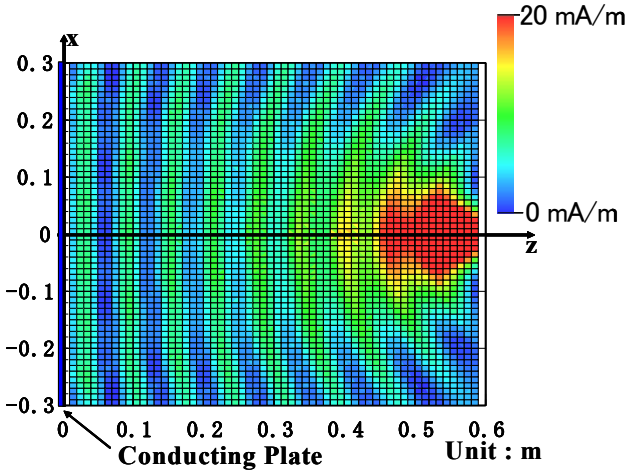

Fig. 12 Magnetic field distribution in xz plane.